Porcine Recombinant Dihydropyrimidine Dehydrogenase: Comparison of the Spectroscopic and Catalytic Properties of the Wild-Type and C671A Mutant Enzymes†

Katrin Rosenbaum,‡ Karin Jahnke,‡ Bruno Curti,§ Wilfred R. Hagen,|| Klaus D. Schnackerz,*,‡ and Maria A. Vanoni§

Theodor-Boveri-Institut für Biowissenschaften, Physiologische Chemie I, Universität Würzburg, Am Hubland, D-97074 Würzburg, Germany, Department of Biochemistry, Agricultural University of Wageningen, NL-6703 HA Wageningen, The Netherlands, and Dipartimento di Fisiologia e Biochimica Generali, Università degli Studi di Milano, Via Celoria 26, 20133 Milano, Italy

Received July 6, 1998; Revised Manuscript Received October 2, 1998

ABSTRACT: Dihydropyrimidine dehydrogenase catalyzes, in the rate-limiting step of the pyrimidine degradation pathway, the NADPH-dependent reduction of uracil and thymine to dihydrouracil and dihydrothymine, respectively. The porcine enzyme is a homodimeric iron−sulfur flavoprotein (2×111 kDa). C671, the residue postulated to be in the uracil binding site and to act as the catalytically essential acidic residue of the enzyme oxidative half-reaction, was replaced by an alanyl residue. The mutant enzyme was overproduced in *Escherichia coli* DH5α cells, purified to homogeneity, and characterized in comparison with the wild-type species. An extinction coefficient of 74 mM^{-1} cm^{-1} was determined at 450 nm for the wild-type and mutant enzymes. Chemical analyses of the flavin, iron, and acid-labile sulfur content of the enzyme subunits revealed similar stoichiometries for wild-type and C671A dihydropyrimidine dehydrogenases. One FAD and one FMN per enzyme subunit were found. Approximately 16 iron atoms and 16 acid-labile sulfur atoms were found per wild-type and mutant enzyme subunit. The C671A dihydropyrimidine dehydrogenase mutant exhibited approximately 1% of the activity of the wild-type enzyme, thus preventing its steady-state kinetic analysis. Therefore, the ability of the C671A mutant and, for comparison, of the wild-type enzyme species to interact with reaction substrates, products, or their analogues were studied by absorption spectroscopy. Both enzyme forms did not react with sulfite. The wild-type and mutant enzymes were very similar to each other with respect to the spectral changes induced by binding of the reaction product $NADP^+$ or of its nonreducible analogue 3-aminopyridine dinucleotide phosphate. Uracil also induced qualitatively and quantitatively similar absorbance changes in the visible region of the absorbance spectrum of the two enzyme forms. However, the calculated K_d of the enzyme−uracil complex was significantly higher for the C671A mutant (9.1 ± 0.7 μM) than for the wild-type dihydropyrimidine dehydrogenase (0.7 ± 0.09 μM). In line with these observations, the two enzyme forms behaved in a similar way when titrated anaerobically with a NADPH solution. Addition of an up to 10-fold excess of NADPH to both dihydropyrimidine dehydrogenase forms led to absorbance changes consistent with reduction of approximately 0.5 flavin per subunit, with no indication of reduction of the enzyme iron−sulfur clusters. Absorbance changes consistent with reduction of both enzyme flavins were obtained by removing $NADP^+$ with a NADPH-regenerating system. On the contrary, the two enzyme species differed significantly with respect to their reactivity with dihydrouracil. Addition of dihydrouracil to the wild-type enzyme species, under anaerobic conditions, led to absorbance changes that could be interpreted to result from both partial flavin reduction and the formation of a complex between the enzyme and (dihydro)uracil. In contrast, only spectral changes consistent with formation of a complex between the oxidized enzyme and dihydrouracil were observed when a C671A mutant enzyme solution was titrated with this compound. Furthermore, enzyme-monitored turnover experiments were carried out anaerobically in the presence of a limiting amount of NADPH and excess uracil with the two enzyme forms in a stopped-flow apparatus. These experiments directly demonstrated that the substitution of an alanyl residue for C671 in dihydropyrimidine dehydrogenase specifically prevents enzyme-catalyzed reduction of uracil. Finally, sequence analysis of dihydropyrimidine dehydrogenase revealed that it exhibits a modular structure; the N-terminal region, similar to the β subunit of bacterial glutamate synthases, is proposed to be responsible for NADPH binding and oxidation with reduction of the FAD cofactor of dihydropyrimidine dehydrogenase. The central region, similar to the FMN subunit of dihydroorotate dehydrogenases, is likely to harbor the site of (dihydro)pyrimidine binding and the FMN cofactor of the enzyme. Two regions containing cysteine residues, which conform to the consensus sequence for the formation of 4Fe-4S clusters, are within the enzyme C-terminal region, while two cysteine-rich regions, conserved in all dihydropyrimidine dehydrogenases and in glutamate synthase β subunits, have been found and may play a role in formation of additional iron−sulfur clusters of dihydropyrimidine dehydrogenases.

10.1021/bi9815997 CCC: $15.00
Published on Web 11/20/1998

Scheme 1

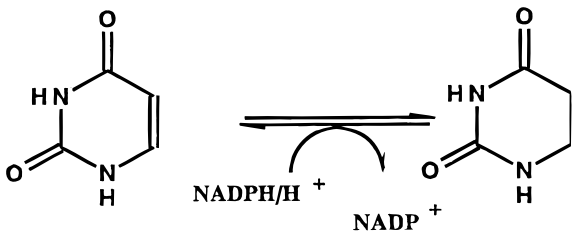

Dihydropyrimidine dehydrogenase (DPD,[1] EC 1.3.1.2) is the first enzyme in the three-step degradation of uracil to *β*-alanine, a putative neurotransmitter. The enzyme catalyzes the NADPH-dependent reduction of pyrimidines to 5,6-dihydropyrimidines, which is the rate-limiting step in the pyrimidine degradation pathway, Scheme 1 (*1*). DPDs were purified from rat (*2*), pig (*3*), bovine (*4*), and human (*5*) liver and from *Alcaligenes eutrophus* (*6*). The cDNA encoding the porcine and human DPD (*7*) has been cloned and sequenced. In humans, DPD is responsible for the rapid degradation of 5-fluorouracil (5-FU), which is widely used in chemotherapy of tumors (*1*). As a consequence of DPD action, high doses of this antitumor drug are administered, causing multiple side effects in the nervous system (*8*). Furthermore, 2-fluoro-*β*-alanine, the end product of the degradative pyrimidine pathway, is a potent neurotoxic agent (*9*). DPD deficiency is an autosomal recessive disorder leading to thymine-uraciluria (*10*), which has been reported to be caused by the deletion of residues 581−635 with no residual enzyme activity (*11*), by a frame-shift mutation (ΔC1897), or by missense mutations with amino acid substitutions at C29R and R886H (*12*). In some patients, DPD deficiency was diagnosed after they had suffered from neurotoxic symptoms during 5-FU treatment (*13*). These patients did not exhibit a characteristic clinical phenotype, although cases in which DPD deficiency is associated with growth and mental retardation have been reported (*14*).

DPD was initially isolated from pig liver by Podschun et al. (*3*). Porcine DPD is composed of two identical subunits of approximately 111 kDa, each carrying one FMN and one FAD cofactor and several iron−sulfur centers. Steady-state kinetic studies of porcine DPD demonstrated a nonclassical two-site ping-pong mechanism (*15*). Thus, separate binding sites are likely to be present for each substrate−product pair, namely, NADPH−$NADP^+$ and uracil−DHU. A scheme has been presented (*15*, *16*) in which NADPH binds to DPD at site 1, where one of the enzyme flavins is located (flavin 1). Electrons are transferred presumably through the iron−sulfur centers of DPD to the flavin (flavin 2) located at site 2 of the enzyme where the pyrimidine substrate binds and is reduced. The pH dependence of the steady-state kinetic parameters of DPD reaction and the study of kinetic isotope effects using stereospecifically deuterated NADPH suggested that NADPH reduction of flavin 1 of DPD is determining the rate of overall turnover of this enzyme (*16*). On the basis of these experiments, an acid−base chemical mechanism was also postulated (*16*). Recently, studies of the reduction of uracil using secondary tritium effects in the presence and absence of solvent deuterium suggested a stepwise reduction of uracil at C-6 followed by protonation at C-5 and a late transition state for this proton transfer step (*17*). At variance with the porcine enzyme, it was proposed that the reaction of bovine DPD is described by a random rapid-equilibrium kinetic mechanism (*18*) where NADPH and uracil independently interact with DPD, and the catalytic turnover is limited by the internal electron transfer between enzymic prosthetic groups.

5-Iodo- (*4*) and 5-ethynyluracil (*19*) were demonstrated to be potent mechanism-based inactivators of bovine DPD. Inactivation of DPD was accompanied by covalent modification of a cysteine residue within a NLSCPHGMGDR tryptic peptide. Such a cysteine residue was proposed to be in the uracil binding site and to play an essential role in catalysis by carrying out acid−base catalysis during uracil reduction.

As the DPD primary structure became available following cloning and sequencing of the corresponding cDNA (*7*), the 5-iodouracil- or 5-ethynyluracil-modified cysteine could be identified as C671 of porcine DPD. Recently, the three-dimensional structure of *Lactococcus lactis* A dihydroorotate dehydrogenase (DHODH-A) was determined (*20*). *L. lactis* DHODH-A is a 33 kDa FMN-containing enzyme, which catalyzes the oxidation of dihydroorotate to orotate and transfers reducing equivalents to quinones. Its aminoacyl sequence is similar to the central region of DPD (residues 527−858), with C130 being the counterpart of C671 of DPD. The three-dimensional structure of DHODH-A clearly showed that C130 is located in the dihydroorotate binding site and is suitably positioned to act as the active site base during dihydroorotate oxidation (*20*).

The cloning of the cDNA of porcine DPD allowed the overproduction of the enzyme in *Escherichia coli* cells and its purification to homogeneity in large quantities (*21*). In this study, we extended the analysis of the primary structure of DPD to tentatively identify the functional regions of the enzyme, and we addressed the role of C671 of porcine recombinant DPD by generating the C671A-DPD mutant enzyme by site-directed mutagenesis. The mutant was overproduced in *E. coli* cells and purified to homogeneity using procedures that yielded the recombinant wild-type DPD (*21*). The C671A-DPD enzyme was essentially inactive in catalytic turnover with NADPH and uracil. Therefore, we studied the effect of the C671A substitution in DPD by monitoring the interaction of several substrates and substrate analogues with C671A-DPD and wild-type DPD by absorbance spectroscopy.

MATERIALS AND METHODS

Chemicals. NADPH and $NADP^+$ were obtained from Boehringer Mannheim or Sigma. Uracil, dihydrouracil (DHU), 3-aminopyridine dinucleotide phosphate (AADP), ADP ribose phosphate, sulfite, and methyl and benzyl

† This work was supported by grants from the Deutsche Forschungsgemeinschaft (to K.D.S.) and from the Ministero dell' Università e della Ricerca Scientifica e Tecnologica, Rome, Italy (to B.C.).

* To whom correspondence should be addressed: Physiologische Chemie I, Biozentrum der Universität Würzburg, Am Hubland, 97074 Würzburg, Germany.

‡ Universität Würzburg.

§ Università degli Studi di Milano.

|| Agricultural University of Wageningen.

[1] Abbreviations: DPD, dihydropyrimidine dehydrogenase; DHODH, dihydroorotate dehydrogenase; DTT, 1,4-dithiothreitol; DEAE, diethylaminoethyl; DHU, 5,6-dihydrouracil; DHO, dihydroorotate; 5-FU, 5-fluorouracil; GltS, glutamate synthase; AADP, 3-aminopyridine dinucleotide phosphate.

viologen were purchased from Sigma. 5-Deaza-5-carbariboflavin was a gift from Dale E. Edmondson (Emory University, Atlanta, GA). All other chemicals were of the highest purity commercially available, and were used without further purification.

Sequence Analysis. The amino acyl sequence of DPD was compared to those of other proteins that could be found in databases (GenBank, EMBL, SwissProt, and PIR) and to those of enzymes using the same or similar substrates and cofactors using programs contained in the GCG Wisconsin package (*22*).

Site-Directed Mutagenesis of the DNA Fragment Encoding Pig DPD. The cDNA fragment encoding pig DPD, cloned into the *Nco*I site of pSE420 (*7*), has been used to overproduce the wild-type form of DPD in *E. coli* DH5α cells (*21*). Such a plasmid was subjected to replacement of nucleotides TG at positions 2011 and 2012 of the insert with nucleotides GC, thus causing the substitution of C671 with an A residue. The Quick Change site-directed mutagenesis kit (Stratagene) was used for the mutagenesis experiment, and mutagenesis conditions were those recommended by the kit manufacturer. The following complementary mutagenesis primers were used (GIBCO BRL): oligo-1, 5′-GGAGTTAAATCTGTCA*GC*TCCACACGGCATGGG-3′; and oligo-2, 5′-CCCATGCCGTGTGGA*GC*TGACAGATTTAACTCC-3′.

Oligo-1 is complementary to residues 1995−2027 of the DPD coding sequence, except for the mutagenesis site (in italic). PCR was carried out using a three-block thermocycler (MWG Biotech). Temperature cycling was carried out as follows: 1 cycle at 95 °C for 30 s and 16 cycles at 95 °C for 30 s, 55 °C for 1 min, and 68 °C for 18 min. The PCR product was treated with *Dpn*I (1 μL, 10 units). The nicked vector DNA incorporating the mutation was then transformed into *E. coli* Epicurian XL1-Blue supercompetent cells (Stratagene). The sequence of one of the clones was checked using an ALF DNA automated sequencer (Pharmacia-LKB) at the Department of Physiological Chemistry I of the University of Würzburg. The plasmid (pC671A) was used to transform *E. coli* DH5α cells for the overproduction of C671A-DPD and for storage of glycerol stocks at −80 °C. Standard DNA manipulations, cell growth, and handling were performed as described by Sambrook et al. (*23*).

The conditions described for the overproduction and purification of recombinant wild-type DPD (*21*) were used for the mutant enzyme. Since no DPD activity in the homogenate was found, chromatography fractions were characterized by SDS electrophoresis (*24*). The resulting enzyme preparation was subjected to gel filtration on Sephadex G-25 PD-10 columns (Pharmacia) equilibrated in 100 mM potassium phosphate buffer (pH 7.3) containing 1 mM DTT and 10% glycerol, concentrated through a centrifugal filter (Biomax-30K, Millipore), and stored in aliquots at −30 °C.

Enzyme Activity and Protein Assays. DPD activity was determined by measuring the initial velocity of NADPH oxidation at 340 nm as described in ref *21*. DPD (4−8.5 μg) and C671A-DPD (45−100 μg) were used to start the assays. One unit of DPD activity is defined as the amount of enzyme which converts 1 μmol of substrate per hour. The protein concentration was determined using the Bio-Rad Protein Assay Reagent (*25*) with bovine serum albumin as the standard protein. A molecular mass of 111 416 Da[2] (*7*) was used to calculate the enzyme concentration.

Iron, Sulfur, and Flavin Analyses. Analyses of the flavin, iron, and sulfur content of the wild type and C671A-DPD were carried out with similar results either directly on preparations obtained at the end of the purification procedure or on protein samples that had been treated in several ways. Aliquots of enzyme solutions (69−178 μM, 80−120 μL) were subjected to gel filtration on Sephadex G-25 columns equilibrated with 10 mM Tris-HCl buffer (pH 7.6). Aliquots (0.5 mL) were collected. DPD-containing fractions were pooled and used to measure the absorbance spectrum, the enzyme activity, the protein concentration, and the flavin, iron, and sulfur content. Loosely bound iron was removed from the protein samples in two different ways. Aliquots of a 100 mM EDTA solution (15 μL) were added to DPD (80−100 μL, 100−137 μM). After incubation on ice, in the dark, for 1 h, the samples were subjected to gel filtration on Sephadex G-25 columns equilibrated with 10 mM Tris-HCl buffer (pH 7.6) or with the same buffer containing 1 mM DTT. The DPD-containing fractions were pooled and analyzed as described above. Alternatively, aliquots (80−100 μL) of DPD solutions were subjected to chromatography on Chelex 100 columns (1 cm × 10 cm), equilibrated with 10 mM Tris-HCl buffer (pH 7.6) or with the same buffer containing 1 mM DTT. Fractions (0.5 mL) were collected, and those containing DPD were pooled and analyzed. Routinely, the iron content of the enzyme preparations was determined using the method of Fish (*26*). For comparison, the method described by Vanoni et al. (*27*) was also used, with similar results. Sulfur analyses were carried out using the method of Rabinowitz (*28*). Identification and quantitation of the FAD and FMN of DPD samples were carried out by reversed phase chromatography in the HPLC apparatus as described in ref *3*. Flavins were extracted by addition of 10% TCA to DPD aliquots (0.9−1.8 mL, 8−20 nM) and incubation for 10 min in the dark. After removal of the denatured protein by centrifugation in a microfuge for 10 min, samples were subjected to chromatography on a Mino RPC-S5/20 HPLC column (Pharmacia, C2/C18, 5 μm; *3*). For routine quantification of the total flavin content, DPD (6.7−12 μM) was denatured in the presence of 10% TCA by heating at 100 °C for 10 min in the presence of light (*27*). Denatured protein was removed by centrifugation in a microfuge for 10 min in the cold. The absorbance spectrum of the supernatant was measured, and an extinction coefficient of 11.1 mM^{-1} cm^{-1} at 446 nm was used to determine the total flavin content of the sample (*29*).

Determination of the Extinction Coefficient of DPD. The absorbance spectra of DPD solutions, which had been pretreated as described above, were recorded. The extinction coefficients at 450 nm were determined by using the enzyme concentration calculated from the protein assay.

Steady-State Kinetic Measurements. Initial velocities of reaction mixtures containing varying amounts of uracil (A) in the presence of constant levels of NADPH (B) were measured at 15, 20, 25, and 30 °C. The reactions were

[2] The calculated mass of the C671A-DPD enzyme is only 32.1 Da lower than that of wild-type DPD. Removal of the initial MA in both protein species by post-translational processing also leads to a negligible decrease in the calculated mass (202.1 kDa).

monitored at 340 nm. After visual inspection of double-reciprocal plots, the data were fitted directly to eq 1, which describes a ping-pong mechanism using the Grafit program (Erythacus Software). Estimates of the maximal velocity (V) and of the K_M values for uracil (K_a) and NADPH (K_b), along with those of the associated errors, were thus obtained.

$$v = (VAB)/(K_aB + K_bA + AB) \quad (1)$$

Spectroscopic Techniques. Absorption spectra were recorded using a Cary 3 spectrophotometer or a model 8452A or 8453 Hewlett-Packard diode array spectrophotometer interfaced with Hewlett-Packard ChemStations. When necessary, the experiments were carried out under anaerobiosis conditions using vessels and procedures described by Williams et al. (*30*). Unless otherwise stated, experiments were carried out at 20 °C in 50 mM potassium phosphate buffer (pH 7.3) containing 1 mM DTT. Substrate solutions were made up fresh in the same buffer. All spectra were corrected for dilution.

The values of fractional absorbance changes at selected wavelengths $[(A_o - A_x)/(A_o - A_f)]$ calculated in the presence of various ligand/enzyme subunit molar ratios (L) during enzyme titrations were used to determine the K_d of the enzyme−ligand complexes. The data were fitted to eq 2 using the Grafit program. The number of binding sites per enzyme subunit (n) and the dissociation constants of the enzyme−ligand complexes were thus determined, along with the associated errors.

$$(A_o - A_x)/(A_o - A_f) = \{-(K_d/[E] + L + n) + \sqrt{[(K_d/[E] + L + n)^2 - 4Ln)]}\}/2 \quad (2)$$

where A_x is the absorbance after a given addition of the ligand, A_o is the initial absorbance of the solution, A_f is the absorbance value at the end of the titration, L is the ligand/enzyme subunit molar ratio, K_d is the dissociation constant of the enzyme−ligand complex, and [E] is the enzyme concentration. The concentrations of the titrating solutions were determined gravimetrically (for dihydrouracil) or spectrophotometrically using published molar extinction coefficients as follows: $NADP^+$ ($\epsilon_{259} = 18\,000\ M^{-1}\ cm^{-1}$), 3-aminopyridine dinucleotide phosphate (AADP, $\epsilon_{331} = 2900\ M^{-1}\ cm^{-1}$; *31*), and uracil ($\epsilon_{259} = 8.12\ M^{-1}\ cm^{-1}$; *32*).

Rapid Reaction Kinetics. The reactivity of wild-type DPD and C671A-DPD with NADPH or with NADPH and uracil was measured anaerobically in a Hi-Tech SF-61 stopped-flow spectrophotometer interfaced with a MacIntosh IIci computer. Data acquisition and analysis were performed using the KISS program (Kinetics Instruments Inc.). Briefly, anaerobiosis in the instrument syringes and plumbing was achieved by flushing them with anaerobic 10 mM sodium dithionite in 50 mM Tris-HCl (pH 8.5), which was allowed to scavenge oxygen overnight. Two hours prior to the beginning of the experiment, the dithionite solution was substituted with anaerobic 50 mM potassium phosphate buffer (pH 7.3) containing 1 mM DTT, 2 mM glucose, and 10 units/mL glucose oxidase from *Aspergillus niger*. Enzyme solutions were made anaerobic in a tonometer by repeated cycles of evacuation and saturation with oxygen-free nitrogen (*30*). Substrate solutions were instead made anaerobic by bubbling oxygen-free nitrogen through them for at least 15 min. For each reaction, equal volumes (70 μL) of enzyme and substrate solutions were rapidly mixed.

RESULTS AND DISCUSSION

Sequence Analysis of DPD. The deduced amino acid sequences of bovine, human, and pig DPD could be retrieved from the GenBank, SwissProt, and PIR databases.[3] The same searches revealed the presence of a putative ORF in the *Caenorhabditis elegans* genome, which would encode a protein similar to mammalian DPD. The primary structures of mammalian DPDs are similar to each other and to the *C. elegans* putative DPD, which has extensions of 37 and 22 residues at the N and C terminus, respectively. From the search for proteins similar to various parts of DPD, it appeared that the protein consists of three parts (Figure 1). As expected from previous studies (*7*, *17*, *20*), the central part of the DPD polypeptide (residues 527−858) is similar to dihydroorotate dehydrogenases, with a higher similarity to those of the B class (*20*; Figure 1). Thus, it should contain the FMN binding site and site 2 of DPD, the site of uracil binding and reduction to dihydrouracil. As detailed in the introductory section, C671 of DPD has its counterpart in C130 of DHODH-A, the residue postulated to be essential for acid−base catalysis in both enzymes. The present databank searches confirmed (*7*) that the C-terminal part of the DPD polypeptide contains two cysteine clusters (residues 953−963 and 986−996) whose spacing is typical of cysteines involved in the formation of ferredoxin-type [4Fe-4S] clusters. Among iron−sulfur clusters containing proteins, the entire C-terminal region of DPD containing such cysteine residues aligns well with the eight-Fe ferredoxin of *Megasphaera elsedenii* (Figure 1). Interestingly, DPD preparations from pig and human livers contained a fraction of partially proteolyzed DPD (*3*, *5*). By comparison of the sequences of such degradation products with those of the DPD polypeptides, it appears that cleavage occurred between residues 903 and 904 of the pig enzyme, within a region connecting the DHODH- and the eight-Fe ferredoxin-like parts of DPD. In light of the similarity shared by the central part of DPD with DHODH-A and the PyrDB subunit of DHODH-B, and of the fact that DPD contains one FAD and uses NADPH, the N-terminal region of DPD was expected to be similar to the *L. lactis* PyrK subunit of DHODH-B. This protein has been recently demonstrated to be a component of the DHODH-B holoenzyme, forming with PyrDB a heterodimer, which is both stable and efficient in catalyzing the oxidation of dihydroorotate to orotate using NAD^+ as the electron acceptor (*33*). PyrK contains one FAD cofactor, one 2Fe-2S center, and the NAD(H) binding site of the DHODH-B holoenzyme. It has been reported (*20*) to

[3] The sequences can be retrieved using the following accession numbers: pig DPD, GenBank U09179; human DPD, PIR A54718; bovine DPD, GenBank U20981; *C. elegans*, GenBank U39742; *Thiobacillus ferrooxidans* GltD, GenBank U36427; *A. brasilense* GltD, SwissProt gltD_azobr; *E. coli* GltD, SwissProt gltD_ecoli; *Pseudomonas aeruginosa* GltS, GenBank U81261; dihydroorotate dehydrogenases from various sources, SwissProt pyrD_*, where * stands for the organism acronym; *L. lactis* dihydroorotate dehydrogenase B, PyrDB subunit, SwissProt pyDB_laclc; *L. lactis* dihydroorotate dehydrogenase A, SwissProt pyDA_laclc; *L. lactis* dihydroorotate dehydrogenase B, K subunit, GenBank X74207; *Megasphaera elsdenii* eight-iron ferredoxin, SwissProt fer_megel.

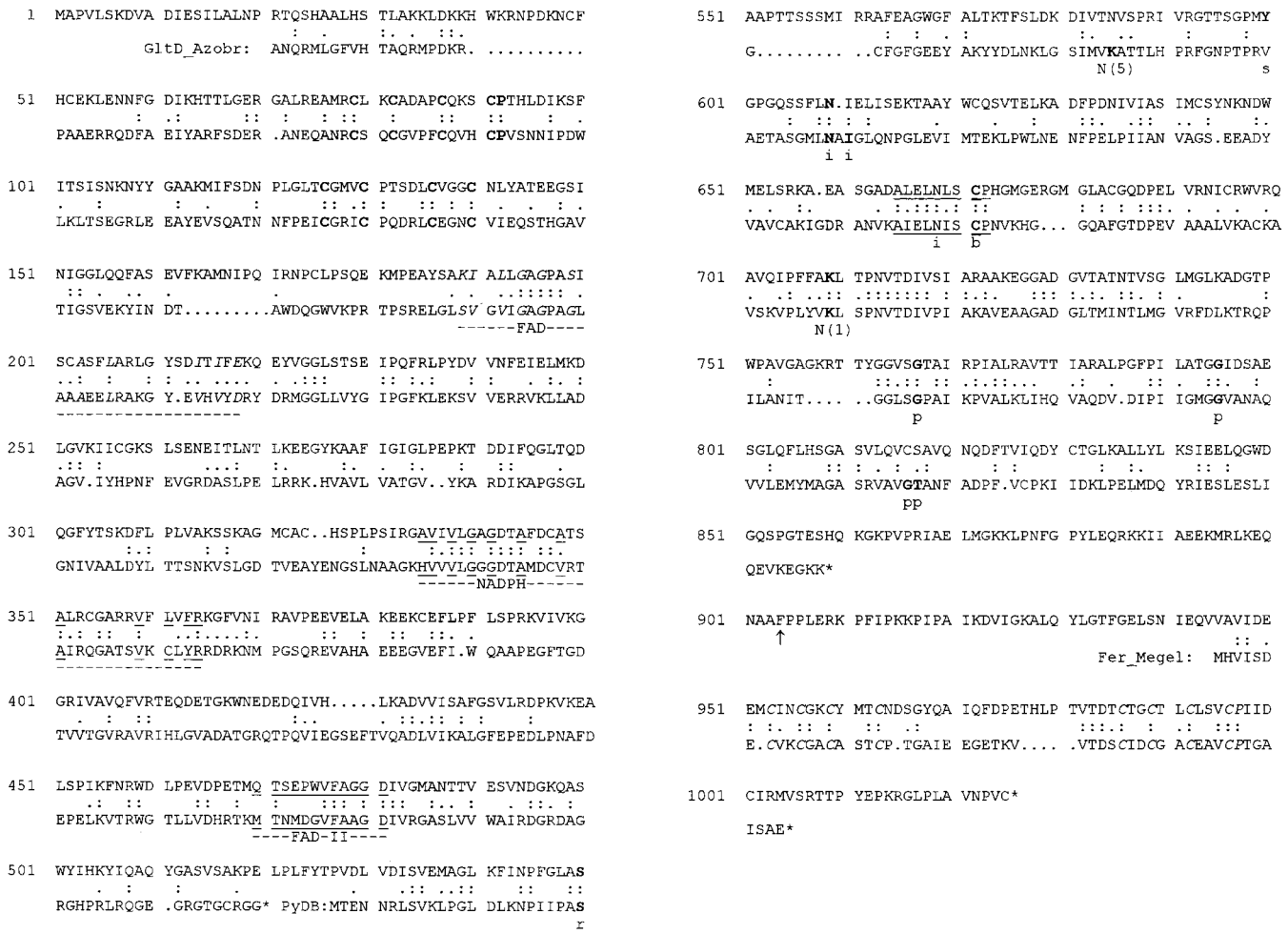

FIGURE 1: Comparison of the primary structure of DPD with those of the GltS β subunit, DHODH, and bacterial eight-iron ferredoxin. The amino acid sequence of DPD (*7*) is compared to those of the β subunit of *A. brasilense* glutamate synthase (GltD_Azobr; *35*), the *L. lactis* DHOD-B PyrDB subunit (PyDB; *33*), and the eight-iron ferrodoxin of *M. elsedenii* (Fer_Megel). Colons indicate identical residues, and dots indicate conserved substitutions according to the following groups of amino acids: A and G; V, I, L, and M; E and D; N and Q; W, F, and Y; S and T; and K and R. For residues 1−520, the conserved cysteine residues found in DPD and in the GltS β subunit are in boldface. The regions corresponding to the adenylate binding region of FAD and NADPH are underlined and labeled. The residues that match the consensus sequence of Wierenga et al. (*44*) are in italic and underlined within the putative FAD and NADPH binding regions, respectively. The region that matches the second FAD consensus sequence as defined by Eggink et al. (*45*) is underlined and labeled. For residues 527−858, residues that in DHODH interact with flavin N-5 and N-1, other positions of the isoalloxazine ring (i), the FMN phosphate group (p), and the active site base (b) are in boldface (*20*). For residues 945−1004, the cysteine residues in the two cysteine-rich regions that match the consensus sequence for the formation of [4Fe-4S] centers are in italic. The arrowhead indicates the position of DPD cleavage that yields the two fragments found in preparations of the enzyme from pig liver (*3*).

be structurally similar to enzymes of the ferredoxin reductase class, in particular, to phthalate dioxygenase reductase (*34*). When the sequence of DPD was compared to those of PyrK, ferredoxin−$NADP^+$ reductase, or phthalate dioxygenase reductase, no significant regions of similarity were detected. The use of BLAST to search for proteins similar to DPD revealed instead a striking similarity of the N-terminal part of DPD (residues 21−520) with the small (β) subunit of bacterial glutamate synthase (GltS) encoded by the *gltD* gene (*35*). Characterization of the recombinant *Azospirillum brasilense* GltS β subunit led to the conclusion that it contains functional site 1 of GltS, the site where NADPH binds and is oxidized with parallel reduction of the FAD cofactor on this subunit (*36*). Thus, it can also be proposed that flavin 1 of DPD is the enzyme FAD cofactor, and that site 1 is contained within the N-terminal domain of this enzyme. Also, interestingly, two cysteine-rich regions of DPD located within positions 79−91 and 126−141 align very well with the N-terminal cysteine-rich regions of GltS β subunit. In GltS, the cysteine residues at the N terminus of the β subunit (residues 47−59 and 94−108) have been proposed to be involved in the formation of the two [4Fe-4S]$^{+/2+}$ clusters of the GltS holoenzyme (*27*, *35*, *37*). The conclusion that DPD contains cysteine-rich regions, which may be involved in the formation of iron−sulfur clusters other than those predicted by the C-terminal [4Fe-4S] cluster signatures, is indeed in line with the iron and sulfur content (≅16 each) reported for DPD from various sources (for a summary, see Table 2 of ref *5*).

Production and Purification of C671A-DPD. The C671A mutant of DPD was obtained by engineering the coding sequence of DPD cloned into plasmid pSE420 (*7*). The mutant enzyme was overproduced in *E. coli* DH5α cells following the protocol that yielded the recombinant wild-type DPD (*21*). The C671A-DPD could be purified in high yield (0.69 mg/g of *E. coli* cell paste) using the purification procedure set up for the recombinant wild-type DPD (*21*). The preparation of C671A-DPD was homogeneous as judged

by SDS electrophoresis, which showed a single protein band with mobility indistinguishable from that of wild-type DPD (not shown). The N-terminal sequences of both the wild type and C671A-DPD were determined. Both enzymes revealed a XVLSKDVADI N-terminal sequence. Thus, both proteins are post-translationally processed in *E. coli* with removal of the MA sequence deduced from analysis of the corresponding cDNA (see Figure 1) to expose a proline residue. N-Terminal sequencing of DPD preparations from pig (*3*) and human (*5*) liver was reported to yield V as the N-terminal residue. The difference between the N-terminal sequence of DPD from natural sources and that of the recombinant species may be due to actual differences in post-translational processing of the protein or to technical reasons. In fact, the identification of the residue released during the first cycle of automated Edman degradation is always difficult, especially when small amounts of protein are being analyzed.

Kinetic Properties of C671A-DPD. C671A-DPD exhibited a specific activity of 0.26 unit/mg under standard activity assay conditions. This value is 1% of that measured for the wild-type enzyme (26 units/mg). The rate of consumption of NADPH in the absence of uracil was 5.7 units/mg, a value greater than 2.1 units/mg which was determined for the wild-type enzyme. The higher NADPH oxidase activity of the mutant with respect to that of wild-type DPD has no obvious explanation. As shown below, major differences in flavin cofactor reactivity can be ruled out. The substitution of C671 with A leads to an essentially inactive enzyme, preventing further steady-state kinetic analyses of the mutant enzyme.

Flavin, Iron, and Sulfur Content of the Wild Type and C671A-DPD and Determination of the Extinction Coefficients. To determine whether the low catalytic activity exhibited by the C671A-DPD mutant enzyme was due to removal of an essential residue or to improper folding or incorporation of the enzyme cofactors, preparations of wild-type DPD and of C671A-DPD were analyzed for their flavin, iron, and sulfur content. Furthermore, the absorbance properties of the preparations were monitored to detect differences between the enzyme species and to determine the DPD extinction coefficient in the visible region.

HPLC analysis of the flavin cofactors released from the enzymes gave 1.0 mol of FAD and 1.0 mol of FMN per mole of the wild-type DPD subunit and 1.1 mol of FAD and 1.0 mol of FMN per mole of the C671A-DPD subunit (Table 1). Chemical analyses of the non-heme iron and acid-labile sulfur content of wild-type DPD and of C671A-DPD were carried out on protein samples obtained at the end of the purification procedure or on samples that were pretreated to remove adventitious iron. Gel filtration, preincubation with EDTA prior to gel filtration, or passage over a Chelex 100 column did not alter the enzyme specific activity, its spectral properties, or its iron and sulfur content. The content of non-heme iron was estimated to be 15.6 and 14.8 mol per mole of the wild-type DPD and C671A-DPD subunit, respectively (Table 1). The amount of acid-labile sulfur for wild-type DPD and C671A-DPD was determined to be 15.7 and 15.6 mol per mole of the enzyme subunit, respectively (Table 1). In these experiments, the subunit concentration was calculated using the protein concentration estimated by the Bradford method. As an internal control of the precision of the protein assay, we recorded the absorbance spectrum of the protein sample under analysis and that of the supernatant obtained after heat denaturation of the enzyme under acidic conditions. Under these conditions, an extinction coefficient at 446 nm of 11.1 mM^{-1} cm^{-1} (*29*) can be used to estimate the total flavin concentration of the sample. As shown in Table 1, the average total flavin content estimated for various enzyme preparations was 1.8 and 1.7 mol per mole of the wild-type DPD and C691A-DPD subunit, respectively. These values are in agreement with the finding of one FAD and one FMN cofactor per enzyme subunit and show that the Bradford protein assay is a reliable method for the determination of DPD concentration. The non-heme iron and acid-labile sulfur content of wild-type DPD and of C671A-DPD are similar to each other and similar to those reported for DPD preparations from pig (*3*) and human (*5*) liver. We attribute the low iron and sulfur content reported previously for recombinant DPD (*21*) to erroneous calculation of the enzyme concentration from protein assays.

Table 1: Determination of the Flavin, Non-Heme Iron, and Acid-Labile Sulfur Content of Wild-Type DPD and C671A-DPD and of the Molar Extinction Coefficients[a]

	DPD	C671A-DPD
FMN[b]	1.0 ± 0.15	1.0 ± 0.17
FAD[b]	1.0 ± 0.10	1.1 ± 0.20
FMN and FAD[c]	1.8 ± 0.13	1.7 ± 0.22
Fe^{2+}	15.6 ± 2.4	14.8 ± 2.0
S^{2-}	16.7 ± 2.6	15.6 ± 2.2
ϵ_{450} (mM^{-1} cm^{-1})	74.6 ± 7.4	73.8 ± 10.7

[a] Analyses were carried out using different preparations of wild-type DPD (*7*) and C671A-DPD (*6*) that had been pretreated as described in Materials and Methods. [b] The flavins were identified and quantified by HPLC. [c] The total flavin content of the preparations was determined from the absorbance spectrum of the supernatant of protein samples that had been denatured by incubation at 100 °C in 10% TCA. The stoichiometries are expresssed as moles per mole of the enzyme subunit.

The absorbance properties of wild-type DPD and C671A-DPD were also similar. The extinction coefficients determined at 450 nm were very similar for the two enzyme species, being 74.7 ± 7.4 and 73.8 ± 10.7 mM^{-1} cm^{-1} for wild-type DPD and C671A-DPD, respectively (Table 1). For practical proposes, in this work, an extinction coefficient at 450 nm of 74 mM^{-1} cm^{-1} was used to calculate the subunit concentration for both wild-type DPD and C671A-DPD. Thus, not only does the C671A-DPD mutant contain the same flavin cofactors and the same number of iron and sulfur atoms as the wild-type form, but also the environment of the flavins and the type of iron−sulfur clusters are apparently similar for the two enzyme species.

With the above information at hand, it could be concluded that the lack of activity of C671A-DPD with NADPH and uracil in kinetic measurements under steady-state conditions is due to the specific removal of C671 from the catalytic center rather than to effects on protein folding, incorporation of the enzyme flavins, or assembly of the enzyme iron−sulfur clusters. For a more detailed characterization of the effects of substitution of C671 with A in DPD, the interaction of the wild type and C671A-DPD with several compounds was studied by absorbance spectroscopy.

Reactivity of the Wild Type and C671A-DPD with Sulfite. Sulfite is commonly employed to probe the environment of flavin cofactors in flavoenzymes (*38*−*40*), since it can form

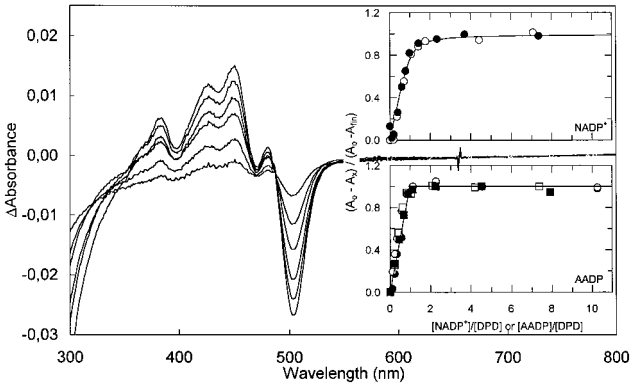

FIGURE 2: Absorbance changes induced by binding of $NADP^+$ and AADP to wild-type DPD and C671A-DPD. (Main panel) Aliquots of $NADP^+$ solutions were added to 6.6 μM solutions of wild-type DPD or C671A-DPD in 50 mM potassium phosphate (pH 7.3) containing 1 mM DTT at 20 °C. The differences between the spectrum of free C671A-DPD and those obtained in the presence of a 0.19-, 0.39-, 0.59-, 0.78-, 0.98-, and 7.36-fold molar excess of $NADP^+$ (from the bottom at 450 nm) are shown. (Top inset) Plot of the fractional absorbance changes observed at 450 nm after a given $NADP^+$ addition as a function of the corresponding $NADP^+$/DPD (○) or $NADP^+$/C671A-DPD (●) molar ratio. The curve shown is that obtained using eq 2 and assuming that one $NADP^+$ binds per DPD subunit with a K_d of 0.47 μM. (Bottom inset) Plot of the fractional absorbance changes observed at 450 nm on addition of AADP as a function of the AADP/DPD molar ratio during the titration of DPD (6.3 μM, ○), C671A-DPD (6.8 μM, ●), DPD (7.1 μM) in the presence of uracil (22.5-fold molar excess, □), and C671A-DPD (6.8 μM) in the presence of uracil (30.8-fold molar excess, ■). The curve indicates tight binding of AADP to each enzyme subunit with a 1/1 stoichiometry.

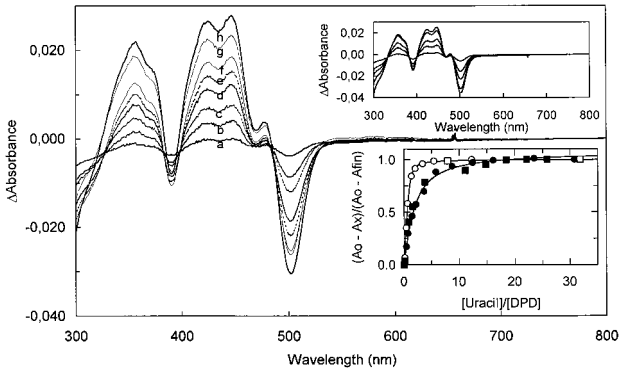

FIGURE 3: Absorbance changes induced by binding of uracil to wild-type DPD and C671A-DPD. Aliquots of uracil solutions were added to solutions of DPD (7.1 μM) or C671A-DPD (6.8 μM) in 50 mM potassium phosphate (pH 7.3) and 1 mM DTT at 20 °C. (Main panel) Differences between the spectrum of C671A-DPD and those obtained in the presence of a 0.145- (a), 0.435- (b), 0.725- (c), 1.45- (d), 2.18- (e), 3.65- (f), 5.85- (g), and 30.8-fold molar excess of uracil (h). (Top inset) Differences between the spectrum of wild-type DPD and those obtained in the presence of a 0.135-, 0.4-, 0.676-, 2.03-, and 22-fold molar excess of uracil (from the bottom at 450 nm). (Bottom inset) Plot of fractional absorbance changes observed at 450 nm in the presence of increasing amounts of uracil during titration of DPD (7.1 μM, ○), C671A-DPD (6.8 μM, ●), DPD (6.3 μM) in the presence of AADP (17.5-fold molar excess, □), and C671A-DPD (6.76 μM) in the presence of AADP (21.7-fold molar excess, ■). The curve through the open symbols was drawn using eq 2 and assuming a 1/1 stoichiometry of uracil binding to wild-type DPD with a K_d of 0.67 μM. The curve drawn through the closed symbols corresponds to that calculated by fitting the data obtained with the mutant enzyme to eq 2 assuming that one uracil binds to one C671A-DPD subunit with a K_d of 9.1 μM.

a covalent adduct with flavin N-5 with well-defined spectral properties. In cases where two flavin cofactors are present in the same enzyme, sulfite reactivity may be a useful tool for distinguishing between them (*27*, *41*) since only one of the enzyme flavins may react with sulfite. Addition of sulfite (up to 32.25 mM) to DPD (6.1 μM) or C671A-DPD (6.7 μM), however, did not cause any spectral changes.

Interaction of Wild-Type DPD and C671A-DPD with $NADP^+$, Pyridine Nucleotide Analogues, and Uracil. On the basis of the two-site model proposed for DPD (*15*, *16*), two distinct binding sites should exist for the interaction with NADPH and uracil. Furthermore, different flavin cofactors should be located at each of the two sites. The hypothesis was made that the effect of the C671A substitution could be studied by monitoring differences in spectral perturbations induced by binding of specific ligands to each of the enzyme subsites. In particular, if C671 were indeed in the uracil site of DPD, one would expect the interaction of the pyridine nucleotides with the two enzyme species to be similar. In contrast, the interactions with uracil or dihydrouracil should be affected by the mutation. Wild-type DPD and C671A-DPD were reacted with $NADP^+$, the nonreducible NADP(H) analogue AADP, and ADP ribose phosphate. $NADP^+$ was added to wild-type DPD or C671A-DPD solutions. The observed absorbance changes were similar for the two enzyme species. They were small, accounting for a maximum 3% decrease of the initial absorbance at 450 nm, but well-defined (Figure 2). The plot of fractional absorbance changes observed at 450 nm versus the $NADP^+$/enzyme molar ratio showed that one $NADP^+$ molecule binds to each DPD subunit (Figure 2, upper inset). The estimated K_d was 0.47 ± 0.14 μM, in agreement with the inhibition constant of 1.0 ± 0.2 μM derived from steady-state kinetic measurements for DPD. The binding of AADP was also studied using both enzyme species. The observed absorbance changes were again qualitatively and quantitatively similar for the two enzymes. They were small (an approximately 3% maximum decrease of absorbance at 450 nm at the end of the titration) but well-defined and similar in shape to those observed with $NADP^+$ (not shown). From the dependence of fractional absorbance changes at 450 nm on the AADP/DPD molar ratio, it was concluded that AADP binds very tightly to both wild-type DPD and C671A-DPD with a 1/1 stoichiometry (Figure 2, bottom inset). An up to 40-fold excess of ADP ribose phosphate did not cause any detectable absorbance changes when added to either DPD species. It should be noted that this pyridine nucleotide analogue indeed binds to DPD, being a competitive inhibitor with respect to NADPH ($K_i = 25 \pm 5$ μM) (*21*). Thus, replacement of C671 with A does not affect binding of pyridine nucleotides to site 1 of DPD as judged by similar perturbations of the flavin absorbance spectrum and dissociation constants for the two enzyme species.

Uracil binding to both enzyme species caused small spectral perturbations (Figure 3) corresponding to an approximately 5% decrease of the initial absorbance at 450 nm. The absorbance changes occurring during uracil titration of DPD were similar to those observed when spectra of DPD and DPD inactivated with 5-iodouracil or 5-iodo-5,6-dihydrouracil were compared (*4*). The absorbance changes observed during the titration of wild-type DPD and of C671A-DPD with uracil were qualitatively similar for the

two enzyme species but different from those observed with $NADP^+$ and AADP (compare Figures 2 and 3). The magnitudes of the maximal absorbance changes at the end of the titration were also similar. However, the dissociation constant of the wild-type DPD−uracil complex, calculated from fractional absorbance changes at 450 nm during the titration, was 0.67 ± 0.09 μM. This value is significantly lower than that determined for C671A-DPD (9.1 ± 0.7 μM, Figure 3). Thus, the C671A mutation in DPD appears to weaken, but not abolish, uracil binding to the enzyme. Furthermore, the mode of binding of uracil to DPD appears to be unaffected by the mutation, as judged by the quality and extent of absorbance changes (Figure 3).

To determine whether the state of occupancy of one site of DPD influences the affinity of the other site for its specific ligand, we carried out a series of titrations of the enzyme−AADP complex with uracil, and of the enzyme−uracil complex with AADP. When AADP was added to DPD or to C671A-DPD in the presence of excess uracil, the absorbance changes were similar to those observed when the free enzyme species were titrated with AADP (data not shown), as were the binding strength and stoichiometry (Figure 2, bottom inset). DPD and C671A-DPD solutions containing excess AADP were titrated with uracil. For both enzyme species, the interaction with uracil was not affected by the presence of AADP with respect to shape, magnitude of the absorbance changes, and K_d values (Figure 3, bottom inset). These data agree well with the presence of two independent sites in DPD for the binding of NADPH and uracil, which must be functionally connected, presumably via at least some of the iron−sulfur centers of the enzyme.

Reactivity of Wild-Type DPD and C671A-DPD with NADPH. To gather preliminary information on the involvement of flavins and iron−sulfur clusters in the DPD reaction, wild-type DPD and C671A-DPD were titrated with NADPH under anaerobic conditions. In agreement with the similar behavior of the two enzyme forms with respect to the binding of $NADP^+$ and AADP, the NADPH titrations of wild-type DPD (not shown) and C671A-DPD (Figure 4) yielded similar results. The observed absorbance changes were complex (main panel of Figure 4) and can be interpreted as the result of partial flavin reduction and of formation of an enzyme−$NADP^+$ complex (Figure 2). If it is assumed that absorbance changes at 450 nm are only due to flavin reduction, and using an extinction coefficient of 10 mM^{-1} cm^{-1} to quantify the flavin being reduced, it could be calculated that 0.54 mol of flavin per mole of DPD subunit was reduced by excess NADPH. A value of 0.6 was obtained with wild-type DPD. Since $NADP^+$ both complicates the interpretation of the spectral changes and may prevent full reduction of the enzyme by binding tightly to DPD (Figure 2), it was removed by adding glucose 6-phosphate and glucose-6-phosphate dehydrogenase from the sidearm of the anaerobic cuvette. A further decrease of absorbance in the 400−500 nm region was observed along with a small increase of the absorbance band in the 500−700 region (Figure 4). From the absorbance changes at 450 nm, approximately 1.8 flavins per wild-type DPD subunit and 1.6 flavins per C671A-DPD subunit were calculated to be reduced in the presence of the NADPH-regenerating system. An estimate of the equilibrium constant for the overall equilibrium (DPD_{ox} + NADPH = DPD_{red} + $NADP^+$) could be obtained from the apparent dissociation

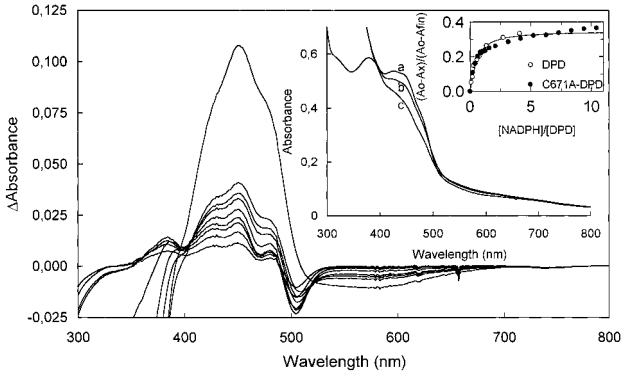

FIGURE 4: Equilibrium NADPH titration of wild-type DPD and C671A-DPD. A solution of C671A-DPD (7 μM) in 50 mM potassium phosphate (pH 7.3) containing 1 mM DTT was made anaerobic (inset, spectrum a). An up to 10.4-fold molar excess of NADPH was added anaerobically from a 0.87 mM NADPH solution (inset, spectrum b). Glucose 6-phosphate (1 μmol) and glucose-6-phosphate dehydrogenase (2 milliunits) were then added from the sidearm of the anaerobic cuvette, and the spectrum was recorded (inset, spectrum c). (Main panel) Differences between the spectrum of C671A-DPD and those obtained in the presence of a 0.2-, 0.4-, 0.6-, 0.8-, 2.1-, 4.2-, 6.3-, and 10.4-fold molar excess of NADPH, and after addition of glucose 6-phosphate and glucose-6-phosphate dehydrogenase (from the bottom at 450 nm). (Top right inset) Plot of fractional absorbance changes observed at 450 nm on addition of NADPH as a function of the NADPH/DPD molar ratio. The final absorbance value at 450 nm (A_{fin}) was that obtained after addition of the NADPH-regenerating system: (○) data obtained with wild-type DPD (6.2 μM) in a similar experiment and (●) data obtained with C671A-DPD (7 μM). The curve shown is that obtained using eq 2, with an n of 0.35 and an apparent K_d of 2.4 μM.

constant of the enzyme−NADPH complex using the data shown in the inset of Figure 4. The apparent K_d value was 2.4 ± 0.25 μM, which is higher than that of the DPD−$NADP^+$ complex (≅0.5 μM) and much higher than that of the DPD−AADP complex (Figure 2, upper inset). The lack of additional information prevents us from elaborating further on the actual meaning of this value. The identity of the species responsible for the absorbance between 500 and 700 nm, which persists after addition of glucose 6-phosphate and glucose-6-phosphate dehydrogenase, remains to be established. In any case, the observed spectral changes do not indicate that the iron−sulfur clusters of DPD are reduced with NADPH to a significant extent.

Reaction of DPD and C671A-DPD with Dihydrouracil. The reactivity of wild-type DPD and of C671A-DPD with DHU was also studied under anaerobic conditions. If C671 was indeed a residue in the (dihydro)uracil binding site of DPD, essential for catalysis, the C671A-DPD would be expected to bind DHU, but no reduction of enzyme flavins should be detected. Addition of DHU to DPD led to small absorbance changes, which could be better analyzed by calculating the differences between the spectrum of the initial (oxidized) enzyme and those obtained after various DHU additions (Figure 5, main panel). The observed absorbance changes were consistent with partial flavin reduction and formation of some DPD−(dihydro)uracil complex. The magnitude of the absorbance changes was also consistent with maximally 0.35 flavin being reduced per DPD subunit, if the total absorbance decrease at 450 nm is due to flavin reduction. Information about the properties of DPD is not sufficient to attempt an interpretation of the negative absor-

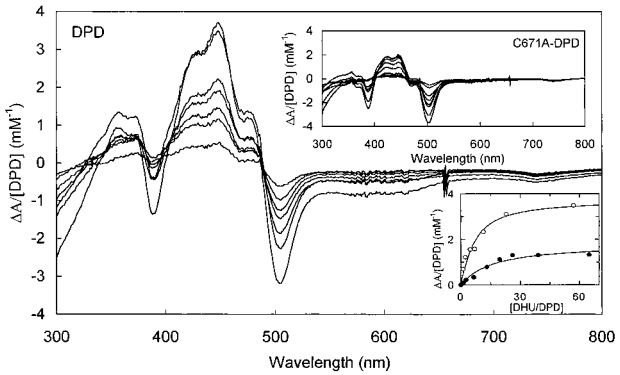

FIGURE 5: DHU titration of wild-type DPD and C671A-DPD. Aliquots of an anaerobic DHU solution (5 mM) were added to anaerobic wild-type DPD (7.0 μM) and C671A-DPD (6.4 μM) in 50 mM potassium phosphate (pH 7.3) and 1 mM DTT at 20 °C. (Main panel) Differences between the spectrum of DPD and those obtained in the presence of a 1.1-, 2.3-, 4.6-, 6.8-, 11.4-, 22.8-, and 56.9-fold molar excess of DHU (from the bottom at 450 nm). (Top inset) Differences between the absorbance spectrum of C671A-DPD and those obtained in the presence of a 1.3-, 2.6-, 6.5-, 13.0-, 19.5-, 26.0-, 39.0-, and 64.9-molar excess DHU (from the bottom at 450 nm). To allow direct comparison, the observed absorbance changes were converted into apparent extinction coefficients. (Bottom inset) Plot of absorbance changes observed at 450 nm on addition of DHU as a function of the DHU/DPD molar ratio. The curve shown for DPD (○) was obtained using eq 2 with an n of 3.75 and an apparent K_d of 34 μM. The curve shown for C671A-DPD (●) was obtained using eq 2 with an n of 1.8 and an apparent K_d of 93.6 μM.

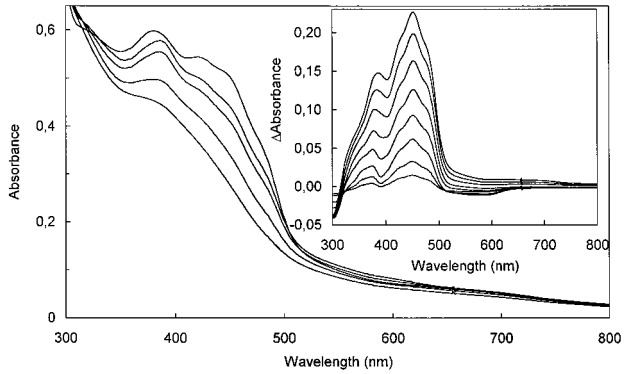

FIGURE 6: Photoreduction of DPD. A solution of DPD (6.4 μM) in 50 mM potassium phosphate (pH 7.3) containing 1 mM DTT, 5 mM EDTA, and 2.75 μM 5-deazaflavin was made anaerobic. Spectra were recorded, before and after irradiation for different times, with a standard slide projector lamp. (Main panel) From the top at 450 nm, spectra of DPD obtained after irradiation for 0, 40, 60, 420, and 3420 s. (Inset) Differences between the spectrum of DPD and those obtained after irradiation for 25, 40, 60, 90, 180, 420, 1620, and 3420 s.

bance band centered around 600 nm in the difference spectra shown in Figure 5. However, the information we obtained by comparing the results of the DHU titration of the wild-type enzyme with those obtained by titrating C671A-DPD was very valuable. Anaerobic titration of C671A-DPD with DHU led to absorbance changes that were qualitatively and quantitatively different from those observed with the wild-type enzyme (Figure 5, upper inset). Less than 2% of the initial absorbance at 450 nm was lost for C671A-DPD as opposed to the 4.3% decrease observed for the wild-type enzyme. The calculated difference spectra (Figure 5, upper inset) did not suggest any flavin reduction. Rather, they were very similar to those observed for the DPD−uracil complex with the exception of a significantly lower differential peak at 350 nm (Figure 3). Fitting of absorbance changes at 450 nm as a function of the DHU/enzyme molar ratio to eq 2 gave apparent K_d values of 34 ± 8.2 and 93.6 ± 28.5 μM for wild-type DPD and C671A-DPD, respectively. While the value for C671A-DPD may reflect the actual dissociation constant of the enzyme−DHU complex, the value calculated for the wild-type form reflects the overall equilibrium between DPD_{ox} and DHU, and DPD_{red} and uracil. As in the case of the titration of DPD with NADPH, no information is available at the present time to draw any conclusion from this value. However, the experiments with DPD and DHU demonstrate that the reaction between DPD and DHU is unfavorable, and that C671A-DPD seems to be unable to transfer reducing equivalents from DHU to the flavin at site 2. Thus, replacement of C671 with A causes weaker binding of uracil and loss of the ability to oxidize DHU. These findings are consistent with the hypothesis that C671 is an essential residue in the interconversion of uracil and dihydrouracil at site 2 of DPD.

Reaction of Photoreduced DPD with Uracil. The reactivity of reduced enzyme with uracil under anaerobic conditions was also studied to determine the effect of the C671A mutation on the DPD reaction. Thus, it was essential to generate reduced DPD. Dithionite was initially chosen as the chemical reductant. However, it was observed that dithionite equilibrated very slowly with wild-type DPD. Even in the presence of methyl and benzyl viologen, equilibration took >60 min after each dithionite addition. Furthermore, dithionite failed to fully reduce DPD, and even at pH values as high as 9.5, it was a poor reductant; equilibration was slow, and a 20-fold molar excess of dithionite was needed to reach maximum absorbance changes. Photoreduction in the presence of 5-deazaflavin (*42*) was instead found to efficiently cause changes in the absorbance spectrum of wild-type DPD (Figure 6) and C671A-DPD (not shown), which were consistent with reduction of both enzyme flavins and at least partial reduction of the enzyme iron−sulfur clusters. Figures 6 and 7 show that the decrease of absorbance at 450 nm, which may be taken as a measure of the overall extent of enzyme reduction, is accompanied by a small increase of absorbance between 500 and 600 nm and negligible changes beyond 650 nm, at early irradiation times. At later reduction stages, the absorbance at long wavelengths decreases. The observed absorbance changes at long wavelengths can be interpreted to be due to formation of a small amount of neutral flavin semiquinone at early irradiation times. Later on, the flavin semiquinone is reduced and reduction of the enzyme iron−sulfur clusters proceeds. Approximately 60 min was required to obtain maximal absorbance changes (Figure 6), while exposure of the enzyme solution to air led to the recovery of the initial enzyme spectrum (not shown). Quantification of the maximum absorbance changes at 450 nm revealed an extinction coefficient of approximately 35.5 mM^{-1} cm^{-1} for both enzyme species. This is certainly consistent with reduction of two flavin cofactors per enzyme subunit (2 × 10 mM^{-1} cm^{-1}) and of several iron−sulfur centers. Accordingly, EPR analyses were carried out on samples of DPD that had been reduced by irradiation in the presence of 5-deazaflavin and EDTA. As observed with samples that had been reduced with excess dithionite (*21*),

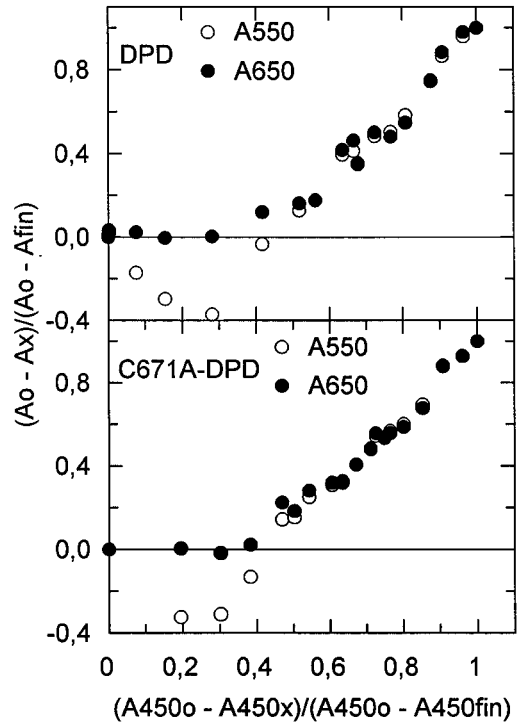

FIGURE 7: Comparison of fractional absorbance changes at various wavelengths during photoreduction of wild-type DPD and C671A-DPD. The fractional absorbance changes observed at 550 and 650 nm during photoreduction of wild-type DPD (6.4 μM, top panel) and C671A-DPD (6.8 μM, bottom panel) are shown as a function of the fractional absorbance changes at 450 nm. Absorbance changes at 650 nm (●) are taken as a measure of the redox state of the enzyme iron−sulfur clusters. Absorbance changes at 550 nm (○) are used as a measure of the formation of neutral flavin semiquinone and reduction of the iron−sulfur clusters. Absorbance changes at 450 nm indicate the overall degree of enzyme reduction.

the preparation exhibited signals consistent with the presence of two [4Fe-4S]$^{+/2+}$ clusters (not shown). However, quantitation of the signal obtained with the photochemically reduced sample of DPD was consistent with the presence of two unpaired electrons per DPD subunit, as opposed to only one calculated for dithionite-reduced DPD (*21*).

Addition of a 15-fold molar excess of uracil, from the sidearm of the anaerobic cuvette, to reduced wild-type DPD led to a partial recovery of absorbance in the visible region (inset of Figure 8). Exposure of the solution to air led to a further increase of the absorbance and to a final spectrum different from that of the initial enzyme preparation. The calculated difference spectra (Figure 8, main panel) clearly showed that the final spectrum was that of the DPD−uracil complex (compare spectra d and e of Figure 8, main panel). Uracil addition to photoreduced C671A-DPD yielded a partial absorbance increase in the visible region (spectrum f of Figure 8), while exposure of the solution to air led to a spectrum similar to that obtained with the wild-type enzyme at the end of the experiment (spectrum 4 of Figure 8). The absorbance change observed on uracil addition was smaller than and different in shape from that observed with the wild-type enzyme, suggesting that C671A-DPD was unable to reduce uracil. However, since trace amounts of oxygen may have been responsible for the observed recovery of absorbance in these experiments, an alternative approach was used to determine which segment of the DPD reaction was affected by the substitution of C671 with A.

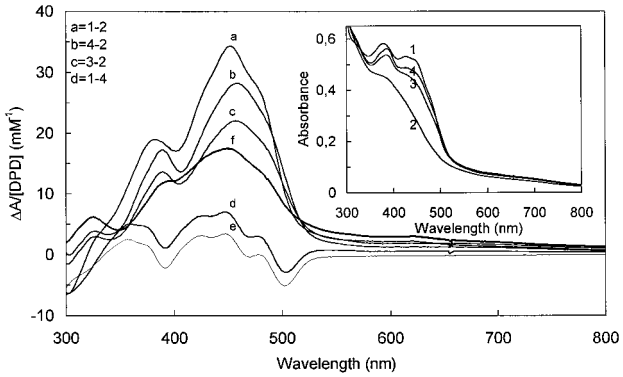

FIGURE 8: Effect of the addition of uracil to photoreduced wild-type DPD and C671A-DPD. A solution of DPD (6.8 μM) in 50 mM potassium phosphate (pH 7.3), 1 mM DTT, 5 mM EDTA, and 2.75 μM 5-deazaflavin was made anaerobic (inset, spectrum 1) and was irradiated for up to 3420 s (inset, spectrum 2). Uracil (15.1-fold molar excess) was added from the sidearm of the anaerobic cuvette (inset, spectrum 3). The cuvette was then opened to air to allow complete reoxidation (inset, spectrum 4). (Main panel) Differences of the spectra of the following enzyme species: spectrum a, DPD_{ox} − DPD_{red}; spectrum b, (DPD_{red} + uracil + oxygen) − DPD_{red}; spectrum c, (DPD_{red} + uracil) − DPD_{red}; and spectrum d, DPD_{ox} − (DPD_{red} + uracil + oxygen). For comparison the difference between the spectrum of DPD and of DPD in the presence of a 22.5-fold molar excess of uracil is shown (spectrum e). Spectrum f is the difference between the spectrum of photoreduced C671A-DPD (6.4 μM) and that obtained after uracil addition (15-fold molar excess). To allow direct comparison, all calculated absorbance differences were converted into apparent extinction coefficients.

Time Course of the Reaction of Wild-Type DPD and C671A-DPD with NADPH in the Absence and Presence of Uracil. The time course of reaction between wild-type DPD and C671A-DPD and NADPH in the absence and presence of excess uracil was measured directly in a stopped-flow spectrophotometer, under anaerobic conditions at 20 °C. The absorbance changes of the solutions were recorded at several wavelengths and were complex, as expected for a complex iron−sulfur flavoprotein. A detailed analysis of the reaction of DPD was outside the scope of this work. However, the data obtained at 450 nm were informative and will be discussed.

The absorbance changes observed during the reaction of wild-type DPD with excess NADPH were qualitatively and quantitatively similar to those obtained with the C671A-DPD mutant (Figure 9). The absorbance decreased to reach a final constant level corresponding to approximately 0.5 flavin being reduced, with most of the absorbance changes occurring at an apparent rate of 0.02 s^{-1}. When wild-type DPD (10.9 μM) was mixed with NADPH (100 μM) and uracil (250 μM), the absorbance at 450 nm decreased to reach a minimum after approximately 0.5 s. After a short plateau, the absorbance increased to a final constant value corresponding to that expected for the formation of complexes of DPD with $NADP^+$ and (dihydro)uracil at the end of the reaction (Figure 9, upper panel).

When C671A-DPD was reacted with NADPH and uracil, the effect of the C671A substitution in DPD was evident. The absorbance at 450 nm decreased to a final minimum level without subsequent absorbance recovery (Figure 9, bottom panel). Thus, the mutant enzyme is essentially unable to react with uracil, as expected from the hypothesis that C671 is a residue essential for the catalysis of uracil reduction at site 2 of DPD.

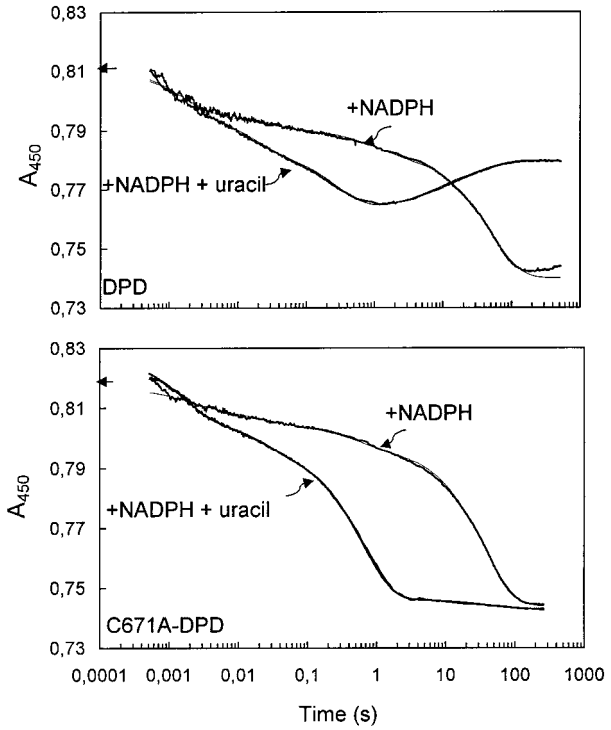

FIGURE 9: Time course of absorbance changes observed during reaction of wild-type DPD and C671A-DPD with NADPH and uracil. Aliquots of DPD (10.9 μM, top panel) or C671A-DPD (11.1 μM, bottom panel) in 50 mM potassium phosphate (pH 7.3) containing 1 mM DTT were reacted with NADPH (100 μM) or with NADPH (100 μM) and uracil (250 μM) in the same buffer, in the stopped-flow apparatus, under anaerobiosis conditions, at 20 °C. The reactions were monitored at 450 nm. The thin lines show the curves which were calculated using the following functions. (Top panel) DPD + NADPH, $A = 0.015 \exp(-600t) + 0.005 \exp(-40t) + 0.0085 \exp(-1.0t) + 0.042 \exp(-0.02t) + 0.74$; DPD + NADPH + uracil, $A = 0.015 \exp(-600t) + 0.013 \exp(-60t) + 0.021 \exp(-3.4t) - 0.008 \exp(-0.164t) - 0.0093 \exp(-0.028t) + 0.78$. (Bottom panel) C671A-DPD + NADPH, $A = 0.007 \exp(-500t) + 0.005 \exp(-48t) + 0.008 \exp(-2.0t) + 0.053 \exp(-0.027t) + 0.744$; C671A-DPD + NADPH + uracil, $A = 0.021 \exp(-648t) + 0.010 \exp(-46t) + 0.050 \exp(-1.56t) + 0.003 \exp(-0.022t) + 0.74$. The arrows indicate the initial absorbance of the wild-type DPD and C671A-DPD solutions.

Interestingly, most of the absorbance changes observed during the reaction of the C671A-DPD mutant with NADPH in the presence of uracil took place at an apparent rate of 1.6 s^{-1}, as opposed to the rate of 0.02 s^{-1} observed during the reaction with NADPH alone. Also during the reaction of wild-type DPD with both NADPH and uracil, most of the absorbance decrease took place with an apparent rate significantly higher than that measured in the presence of NADPH alone (3.4 s^{-1}, Figure 9, top panel). Only in the presence of uracil is the value of the apparent rate of reduction of DPD by NADPH higher than the turnover number determined for wild-type DPD at 20 °C (0.58 s^{-1}, Figure 9, top panel). Therefore, these experiments also show that uracil has a dramatic effect on the rate at which NADPH reacts with DPD and that the C671A-DPD mutant may be the ideal system for studying such an effect in detail.

CONCLUSIONS

The main goal of this work was the determination of the role of C671 in the catalysis of DPD. This residue was postulated to be essential for reduction of uracil at site 2 of DPD. C671A-DPD was overproduced, purified to homogeneity, and found to be essentially inactive during turnover with NADPH and uracil, as measured under steady-state conditions. Thus, the characterization of the mutant enzyme was carried out by comparing the absorbance properties of wild-type DPD and C671A-DPD at equilibrium and in the stopped-flow spectrophotometer. The results demonstrate that substitution of an alanyl residue for C671 does not affect the properties of site 1 of DPD, the site where NADPH binds and is oxidized with concomitant reduction of the flavin cofactor located at this site (flavin 1). The binding interactions between DPD and NADP(H) analogues are in fact indistinguishable for wild-type and mutant enzyme species, as is the time course of absorbance changes observed during the reaction of the enzymes with NADPH. The C671A substitution weakens, but does not abolish, the binding of uracil to site 2 of DPD. However, DHU is unable to cause any flavin reduction in the mutant enzyme, and uracil is no longer able to oxidize the NADPH-reduced enzyme, as observed in the stopped-flow apparatus. Thus, C671 appears to be a catalytically essential residue at site 2 of DPD. It should be noted that, as this work was being completed, the C130 mutant of DHODH-A was produced and characterized and this residue shown to be also essential for dihydroorotate oxidation (*43*). In C130S-DHODH-A, an increase in activity was observed at high pH values, suggesting that the serine hydroxyl group may dissociate and substitute to some extent for the C130 thiolate during catalysis.

This study also yielded valuable information about wild-type DPD. The extinction coefficient of DPD was determined to be approximately 74 mM^{-1} cm^{-1}, a value greater than that previously reported for the enzyme from bovine liver (31 mM^{-1} cm^{-1}; *4*). It was demonstrated that both recombinant enzyme species exhibit flavin, iron, and acid-labile sulfur contents similar to those of the pig and human liver enzymes (*3*, *5*): one FAD, one FMN, approximately 16 non-heme iron atoms, and 16 acid-labile sulfur atoms per enzyme subunit (Table 1). The high iron and sulfur content is consistent with the finding of two cysteine-rich regions at the N terminus of DPD, in addition to those already detected at the C terminus. The entire N-terminal region was found to be similar to the GltS β subunit, which was shown to harbor site 1 of GltS, another complex iron−sulfur flavoprotein (*36*). At this site, NADPH binds and is oxidized with electron transfer to the FAD cofactor in this subunit. The similarity of the central part of DPD with enzymes of the DHODH class was previously detected (*17*, *20*). Thus, it can be proposed that site 1 of DPD may be within its N-terminal region and that FAD is flavin 1 of DPD. Flavin 2 may be the FMN cofactor of DPD, located in the central part of the polypeptide, which harbors site 2 of DPD.

None of the experiments presented here give definitive information on the type and number of the enzyme iron−sulfur clusters or on their role in catalysis. Dithionite was found to be a slow poor reductant of DPD, thus explaining the failure to achieve a significant degree of reduction of DPD iron−sulfur centers during preliminary experiments (*21*). In this work, photochemical reduction of DPD was found to be more effective than dithionite reduction. EPR spectroscopy experiments have been carried out on DPD samples that had been incubated with NADPH alone or that have been photoreduced. Only photoreduction yielded an

EPR-active species. The observed signals were similar to those reported previously for a dithionite-reduced sample (*21*), but quantification was consistent with two unpaired electrons per DPD subunit as opposed to only one obtained on dithionite reduction. Thus, it appears that DPD iron−sulfur clusters exhibit unusually low oxidoreduction potentials and/or spectroscopic properties, which are currently under investigation.

The equilibrium binding studies confirmed the presence of distinct sites for the pyridine nucleotide and the uracil substrates. We confirmed that (*15*, *18*) the state of occupancy of one site does not affect the binding interaction of the other with its specific ligand. However, monitoring the absorbance changes during reaction of DPD with NADPH, alone or in the presence of uracil directly in the stopped-flow apparatus, revealed an unexpected effect of uracil in accelerating the reduction of DPD by NADPH. Thus, analysis of DPD by the variety of approaches used in this work revealed that the enzyme has a degree of complexity that is greater than expected, but also provided a set of information on which to build future studies of this enzyme.

REFERENCES

1. Wasternack, C. (1980) *Pharmacol. Ther. 8*, 629−665.
2. Shiotani, T., and Weber, G. (1981) *J. Biol. Chem. 256*, 219−224.
3. Podschun, B., Wahler, G., and Schnackerz, K. D. (1989) *Eur. J. Biochem. 185*, 219−224.
4. Porter, D. J. T., Chestnut, W. G., Taylor, L. C. E., Merill, B. M., and Spector, T. (1991) *J. Biol. Chem. 266*, 19988−19994.
5. Lu, Z. H., Zhang, R., and Diasio, R. (1992) *J. Biol. Chem. 267*, 17102−17109.
6. Schmitt, U., Jahnke, K., Rosenbaum, K., Cook, P. F., and Schnackerz, K. D. (1996) *Arch. Biochem. Biophys. 332*, 175−182.
7. Yokota, H., Fernandez-Salguerno, P., Furuya, H., Lin, K., McBride, O. W., Podschun, B., Schnackerz, K. D., and Gonzalez, F. J. (1994) *J. Biol. Chem. 269*, 23192−23196.
8. Hull, W. E., Port, R. E., Hermann, R., Britsch, B., and Kunz, W. (1988) *Cancer Res. 48*, 1680−1688.
9. Okeda, R., Shibutani, M., Matsuo, T., Kuroiwa, T., Shimokawa, R., and Tajima, T. (1990) *Acta Neuropathol. 81*, 66−73.
10. Bakkeren, J. A. J. M., De Abreu, R. A., Sengers, R. C. A., Gabreels, F. J. M., Mass, J. M., and Renier, W. O. (1984) *Clin. Chim. Acta 140*, 247−256.
11. Vreken, P., van Kuilenburg, A. B. P., and Meinsma, R. (1996) *J. Inherited Metab. Dis. 19*, 645−646.
12. Vreken, P., van Kuilenburg, A. B. P., Meinsma, R., and van Gennip, A. H. (1997) *J. Inherited Metab. Dis. 20*, 335−338.
13. Tuchman, M., Stoeckeler, J. S., Kiang, D. T., O'Dea, R. F., Rammaraine, M. L., and Mirkin, B. L. (1985) *N. Engl. J. Med. 313*, 245−249.
14. Berger, R., Stoker-de Vries, S. A., Wadman, S. K., Duran, M., Beemer, F. A., de Bree, P. K., Weits-Binnerts, J. J., Penders, T. J., and van der Woude, J. K. (1984) *Clin. Chim. Acta 141*, 227−234.
15. Podschun, B., Cook, P. F., and Schnackerz, K. D. (1990) *J. Biol. Chem. 265*, 12966−12972.
16. Podschun, B., Jahnke, K., Schnackerz, K. D., and Cook, P. F. (1993) *J. Biol. Chem. 268*, 3407−3413.
17. Rosenbaum, K., Jahnke, K., Schnackerz, K. D., and Cook, P. F. (1998) *Biochemistry 37*, 9156−9159.
18. Porter, D. J. T., and Spector, T. (1993) *J. Biol. Chem. 268*, 19321−19327.
19. Porter, D. J. T., Chestnut, W. G., Merril, B. M., and Spector, T. (1992) *J. Biol. Chem. 267*, 5236−5242.
20. Rowland, P., Nielsen, F. S., Jensen, K. F., and Larsen, S. (1997) *Structure 5*, 239−252.
21. Rosenbaum, K., Schaffrath, B., Hagen, W. R., Jahnke, K., Gonzalez, F. J., Cook, P. F., and Schnackerz, K. D. (1997) *Protein Expression Purif. 10*, 185−191.
22. Devereux, J., Haeberli, P., and Smithies, O. (1984) *Nucleic Acids Res. 12*, 387−395.
23. Sambrook, J., Fritsch, E. F., and Maniatis, T. (1989) in *Molecular Cloning: A laboratory manual*, 2nd ed., Cold Spring Harbor Laboratory Press, Cold Spring Habor, NY.
24. Laemmli, U. K. (1970) *Nature 227*, 680−685.
25. Bradford, M. M. (1976) *Anal. Biochem. 72*, 248−254.
26. Fish, W. W. (1988) *Methods Enzymol. 158*, 375−364.
27. Vanoni, M. A., Edmondson, D. E., Zanetti, G., and Curti, B. (1992) *Biochemistry 31*, 4613−4623.
28. Rabinowitz, J. C. (1978) *Methods Enzymol. 53*, 275−277.
29. Hinkson, J. W. (1968) *Biochemistry 7*, 2666−2672.
30. Williams, C. H., Arscott, L. D., Matthews, R. G., Thorpe, C., and Wilkinson, K. D. (1979) *Methods Enzymol. 62*, 185−198.
31. Anderson, B. M., and Fischer, T. L. (1980) *Methods Enzymol. 66*, 81−87.
32. Sober, H. A., Harte, R. A., and Sober, E. K. (1970) in *Handbook of Biochemistry*, 2nd ed., The Chemical Rubber Co., Cleveland, OH.
33. Nielsen, F. S., Andersen, P. S., and Jensen, K. F. (1996) *J. Biol. Chem. 271*, 29359−29365.
34. Gassner, G. T., Ludwig, M., Gatti, D. L., Correll, C. C., and Ballou, D. P. (1995) *FASEB J. 9*, 1411−1418.
35. Pelanda, R., Vanoni, M. A., Perego, M., Piubelli, L., Galizzi, A., Curti, B., and Zanetti, G. (1993) *J. Biol. Chem. 268*, 3099−3106.
36. Vanoni, M. A., Verzotti, E., Zanetti, G., and Curti, B. (1996) *Eur. J. Biochem. 236*, 937−946.
37. Vanoni, M. A., Fischer, F., Ravasio, S., Verzotti, E., Edmondson, D. E., Hagen, W. R., Zanetti, G., and Curti, B. (1998) *Biochemistry 37*, 1828−1838.
38. Müller, F., and Massey, V. (1969) *J. Biol. Chem. 244*, 4007−4016.
39. Massey, V., Müller, F., Feldberg, R., Schuman, M., Sullivan, P. A., Howell, L., Mayhew, S. G., Matthews, R. G., and Foust, G. P. (1969) *J. Biol. Chem. 244*, 3999−4006.
40. Massey, V., and Hemmerich, P. (1980) *Biochem. Soc. Trans. 8*, 246−257.
41. Jorns, M. S. (1985) *Biochemistry 24*, 3189−3194.
42. Massey, V., and Hemmerich, P. (1978) *Biochemistry 17*, 9−17.
43. Björnberg, O., Rowland, P., Larsen, S., and Jensen, K. F. (1997) *Biochemistry 36*, 16197−16205.
44. Wierenga, R. K., DeMayer, M. C. H., and Hol, W. G. J. (1985) *Biochemistry 24*, 1346−1357.
45. Eggink, G., Engel, H., Vriend, G., Terpstra, P., and Witholt, B. (1990) *J. Mol. Biol. 212*, 135−142.

BI9815997